Published in final edited form as:

Mol Microbiol. 2008 March ; 67(6): 1184–1195. doi:10.1111/j.1365-2958.2008.06120.x.

Novel ultrastructures of *Treponema primitia* and their implications for motility

Gavin E. Murphy[1], **Eric G. Matson**[2], **Jared R. Leadbetter**[2], **Howard C. Berg**[3], and **Grant J. Jensen**[1,*]

[1]Division of Biology, California Institute of Technology, Pasadena, CA 91125, USA.

[2]Division of Environmental Science and Engineering, California Institute of Technology, Pasadena, CA 91125, USA.

[3]Department of Molecular and Cellular Biology, Harvard University, Cambridge, MA 02138, USA.

Summary

Members of the bacterial phylum *Spirochaetes* are generally helical cells propelled by periplasmic flagella. The spirochete *Treponema primitia* is interesting because of its mutualistic role in the termite gut, where it is believed to cooperate with protozoa that break down cellulose and produce H_2 as a by-product. Here we report the ultrastructure of *T. primitia* as obtained by electron cryotomography of intact, frozen-hydrated cells. Several previously unrecognized external structures were revealed, including bowl-like objects decorating the outer membrane, arcades of hook-shaped proteins winding along the exterior and tufts of fibrils extending from the cell tips. Inside the periplasm, cone-like structures were found at each pole. Instead of the single peptidoglycan layer typical of other Gram-negative bacteria, two distinct periplasmic layers were observed. These layers formed a central open space that contained two flagella situated adjacent to each other. In some areas, the inner membrane formed flattened invaginations that protruded into the cytoplasm. High-speed light microscopic images of swimming *T. primitia* cells showed that cell bodies remained rigid and moved in a helical rather than planar motion. Together, these findings support the 'rolling cylinder' model for *T. primitia* motility that posits rotation of the protoplasmic cylinder within the outer sheath.

Introduction

Many members of the phylum *Spirochaetes*, such as *Treponema pallidum*, *Leptospira interrogans* and *Borrelia burgdorferi*, are important human pathogens, causing syphilis, Weil's disease and Lyme disease respectively. Others, however, cooperate beneficially with their animal hosts. *Treponema primitia*, for example, is a species that inhabits the hindgut of

*For correspondence. Jensen@caltech.edu; Tel. (+1) 626 395 8827; Fax (+1) 626 395 5730.

Supplementary material

This material is available as part of the online article from: http://www.blackwell-synergy.com/doi/abs/10.1111/j.1365-2958.2008.06120.x

(This link will take you to the article abstract).

Please note: Blackwell Publishing is not responsible for the content or functionality of any supplementary materials supplied by the authors. Any queries (other than missing material) should be directed to the corresponding author for the article.

the termite *Zootermopsis angusticolis* and synthesizes acetate, the major energy source of their insect host, from the H_2 and CO_2 generated by protozoa during the fermentation of wood polysaccharides (Breznak and Switzer, 1986; Leadbetter *et al*., 1999; Graber *et al*., 2004; Warnecke *et al*., 2007). In early microscopic studies on termite gut ecosystems, spirochetes were observed to attach to, and sometimes even propel, certain hindgut flagellate protozoa (Cleveland and Grimstone, 1964; Bloodgood and Fitzharris, 1976; Holt, 1978). It has since been hypothesized that interspecies H_2 transfer between H_2-producing protozoa and H_2-consuming spirochetes such as *T. primitia* might be promoted by such associations (Bloodgood and Fitzharris, 1976).

Spirochetes are unusual with respect to other bacteria in that their flagella are confined within the periplasm. The rotation of periplasmic flagella (PF) is thought to drive motility by causing the entire cell body to bend (*B. burgdorferi*), gyrate (*L. interrogans*) and/or rotate (*Cristispira balbianii* and *Spirocheta aurantia*) (Berg, 1976; Berg *et al*., 1978; Goldstein and Charon, 1988; 1990; Goldstein *et al*., 1994; 1996). Compared with externally flagellated bacteria, spirochetes excel in gel-like, viscous environments (Berg and Turner, 1979; Nakamura *et al*., 2006). Motility has been linked to spirochete pathogenesis (Li *et al*., 2001) and in *T. primitia*, it is probably vital for its role in the termite gut.

Most of what is known about spirochete cell structure comes from conventional electron miscroscopic studies, which involve chemical fixation, dehydration, plastic embedding, sectioning and heavy metal staining. While some details are lost or distorted by these procedures, they have revealed inner and outer membranes, subterminally attached PF and close associations with host protozoa (Holt, 1978). More recently, it has become possible to image intact cells in three dimensions (3-D) in a nearly native state by electron cryotomography (ECT) (Lucic *et al*., 2005; Jensen and Briegel, 2007). In this technique, cells are spread into thin films and frozen so quickly that ice crystals do not form, thus preserving the specimen in a life-like, ‘frozen-hydrated’ state. A series of images are then recorded of each frozen cell as it is rotated incrementally in an electron microscope. The images are used to calculate a 3-D reconstruction of the entire cell and its contents with a resolution that is typically sufficient to identify and locate large macromolecular complexes *in situ*. The first structure of a complete bacterial flagellar motor, for instance, was obtained by imaging *T. primitia* cells this way (Murphy *et al*., 2006). Previous tomographic reconstructions of the spirochete *Treponema phagedenis* cells have already shown their interesting cytoskeletal architecture, although these cells were conventionally preserved rather than frozen-hydrated (Izard *et al*., 2004).

By imaging *T. primitia* cells in a frozen-hydrated state by ECT, here we report the discovery of several ultrastructural features including bowls, arches and fibrils on the outer surface; a multi-layered and capped periplasmic space; and a subdivided cytoplasm with internal membrane sacs and other large structures. Together with high-speed, light microscopic video of swimming *T. primitia* cells, these findings are consistent with the ‘rolling cylinder’ model of spirochete motility, wherein the PF cause a cell’s protoplasmic cylinder (PC) to rotate within its outer sheath (OS) (Berg, 1976).

Results

Treponema primitia cells were plunge-frozen in thin films of culture media across EM grids and imaged tomographically. Eighteen 3-D reconstructions were calculated that together included one complete cell and 23 cell tips (one reconstruction contained a complete cell, six contained two cell tips and 11 contained single tips). Figure 1 shows a tomographic slice through the tip of one representative reconstruction (arbitrarily referred to as cell #1). Several novel features were observed, including structures we refer to here as 'surface bowls', 'surface hook arcades', 'polar fibrils' and a polar 'cone' inside the periplasm. Two flagella and a flagellar motor were also seen, as expected. Ribosome-like particles were visible in the cytoplasm. The cell's diameter was ~350 nm.

In order to clarify the structures of the various features, several cells were manually segmented (i.e. voxels were subjectively designated as parts of specific structures, rendered in different colours and viewed in 3-D). Views of the manually segmented cell #1 are shown in Fig. 2 and Movie S1. Because in ECT, samples can only be tilted to ~65°, surfaces parallel to the grid, like the tops and bottoms of the cells, were difficult to resolve, and so were not segmented. In the segmented model of cell #1, the flagella and hook arcades were seen to wrap with a left-handed twist about the cell, and the two flagella lay side by side directly beneath the surface hook arcade. One flagellum (coloured red) extended from its motor ~100 nm away from the cell tip to the edge of the reconstruction. The second flagellum (coloured green) must have traversed nearly the entire length of the cell, as it presumably emerged near the opposite cell pole, and was seen here to terminate just 500 nm away from the reconstructed tip.

Connected cells were also seen (Fig. 3 and Movie S2). Motile chains of what appeared to be two, four or even eight cells were also seen by light microscopy. Because these chains were more common in log phase than stationary phase cultures, they were likely to be dividing. Long chains were also found in unshaken cultures in low-viscosity media, suggesting that some mechanical stress in the environment or perhaps the twist that might naturally arise from swimming in viscous media might help cells separate.

External structures

Novel 'surface bowls' were present on the outer membranes of all the cells. While they usually appeared to be randomly arranged, in one case they formed two or three rows of left-handed spirals (Fig. 3G). Sometimes the bowls were present underneath the surface hooks (Figs 2B, 5A and B). Fifty-six individual bowls were computationally extracted, aligned, averaged and circularly symmetrized to produce a higher signal-to-noise density map (Fig. 4). The bowls were 16 nm high, 45 nm wide, and their bottoms were 8 nm away from the membrane (measured from the centre of each feature). In the symmetrized average, the membrane just below the bowl appeared 'dimpled' (Fig. 4D), but this was likely just an artefact of the microscope's point-spread function, which causes a reverse-contrast fringe, or 'halo' around dense objects. In this case, the halos around the bowl and the membrane are predicted to have reduced the apparent density of the top of the membrane, the bottom of the bowl and the 'stalk' that connects them.

Long series of arches (arcades) were seen decorating the outside of 18 of the 24 partially or fully reconstructed cells. In the best-preserved cells, the arcades followed a left-handed path. In cell #1, for instance, an arcade began over the motor and apparently wrapped around the cell directly above the flagella along the entire reconstructed region (Fig. 2, and B in particular). There were four arcades on cell #2a and a partial arcade on cell #2b. A pair of arcades ran above cell #2a's flagella, but it did not wrap directly over them (Fig. 3D–F). Another arcade was located a quarter arc away from the flagella, and the fourth was located opposite the flagella. The possible relationship between the arcades and the flagella in general was puzzling. In many cases, there were arcades on cell surfaces far away from the flagella, and most of the flagella were not covered by arcades, but there were a few noteworthy instances where the hook arcades were seen directly over the flagella for long distances, as if they were associated (as in cell #1).

Figure 5 highlights a pair of ~600-nm-long arcades that ran atop cell #3 approximately above two flagella. These arcades were particularly well resolved because the outer membrane of this cell was ruptured and slightly detached, but the typically left-handed trajectory appears to have been distorted. The arches appeared to be composed of two symmetric hooks that joined at the top. Several sections of a hook arcade were aligned together and averaged, then positioned onto their probable twofold symmetry axis. The average (Fig. 5D) shows the meeting of individual hooks at the top, where adjacent arches touched each other to form a continuous roof. The hooks were ~4 nm thick; the pillars were 29 nm apart; the arcades were 40 nm wide and 43 nm high; and the arches were seen to be angled 35° from the long axis of the arcade, so that each arch was formed by hooks offset by two positions along the long axis of the arcade (Fig. 5E). The pillars were not visible in the average because their densities were either weak and/or non-uniform.

Tufts of 6-nm-thick fibrils extended from the tips of 22 of the cells (Fig. 6), including both poles of cell #6 (Fig. 6G). Some tips had one tuft (Figs 3, 6A–D and G), others two (Figs 2 and 6E), and still others had forked tufts (Fig. 6H). Some fibrils were short and fairly straight, and others were long and curved. Because the longest straight fibril was 350 nm and the shortest curved fibril was 370 nm, however, it is possible that they were all fundamentally the same, but the fibrils' persistence length was only a few hundred nanometres. Both straight and curved fibrils were seen bundled together in the same tuft. An exceptional 1.6-μm-long fibril was seen on cell #1 (Fig. 6E). In some cases, density could be traced from the fibrils through the periplasmic cone all the way to the inner membrane (Fig. 6C).

Internal structures

Apparently porous, cone-shaped structures were present at the periplasmic tips of all but one of the reconstructed cells (Fig. 7 and Movie S3). The cones lay underneath the outer membrane region from which the fibrils extended. In the two reconstructions of connected cells, each cell had its own periplasmic cone, and the two cones abutted tip to tip.

Two layers of density were visible between the inner and outer membranes in some reconstructions (Fig. 8A and Movie S4). To measure the distances between the elements of the cell wall, density profiles along normals to the outer membrane were calculated and

averaged in regions where the periplasm was nearly uniformly thick (Fig. 8E). This excluded the area around flagella and especially the flagellar motor, where the periplasm was wider (visible in Figs 8C and 1A). Four peaks emerged, corresponding, respectively, to the outer membrane at the top/origin, an ‘outer periplasmic layer’ 9 nm into the periplasm, an ‘inner periplasmic layer’ 12 nm further down and finally the inner membrane another 7 nm nearer the centre of the cell. Because distances were measured with respect to the outer membrane, variations in the thickness of the periplasm increasingly blurred features towards the interior, so that the peaks corresponding to the inner membrane and inner periplasmic layers appeared broader than their outer counterparts. The flagella were 20 nm thick, and in some views were clearly seen to lie between the two periplasmic layers, pushing them apart (see also Movie S4).

Flattened membrane sacs were visible in several reconstructed cells. They were always close to the inner membrane and appeared to be membrane invaginations (Fig. 9). Inside the inner membrane, the cytoplasm was clearly and consistently partitioned into two regions with different textures: a cylindrical, outer shell punctuated by numerous ribosome-like particles and a smoother, inner tube devoid of ribosome-like particles which was presumably filled by the genome (Fig. 9A). Spherical bodies ~30 nm wide with smooth and uniform internal textures reminiscent of polymer storage granules were seen in the cytoplasm of several of the cells (Fig. 7C). Ordered arrays resembling the structures previously reported to be chemotaxis receptor arrays were also present just below the inner membrane close to the flagellar motors at the cell poles (Fig. 9A) (Lefman *et al*., 2004; Zhang *et al*., 2004).

Swimming behaviour

In order to gain insight into the possible functions of some of these ultrastructural features, high-speed movies were recorded of cells swimming in a buffered salt solution containing 0.175% methyl cellulose (viscosity = 4 cP), which is only slightly more viscous than water (Fig. 10 and Movie S5). Because motility models for other spirochetes, such as *Leptospira*, depend on gyrations of polar hooks, we looked carefully for evidence of any such changes in the shape of the cell, but none was seen. The cells were also clearly not planar waves, like *Borrelia*, which appear as straight lines sometimes, and then later as sine waves of varying amplitude as the plane of the wave rotates with respect to the beam. *T. primitia* cells instead looked like rigid helices at all times. Because the relative height of each section along the cell was discernible by the sharpness of its focus, points of similar focus were seen to move steadily down the cell (Fig. 10, arrowheads). By marking the glass coverslip above the cells and noting which points on fixed and non-motile cells were ‘higher’ and ‘lower’ in the microscope, the cells were seen to be left-handed helices. The helical pitch (wavelength) of the cell was ~2.5 μm, the radius was ~0.6 μm and the cell moved at ~12 μm s^{-1}. In Fig. 10, it can be seen that a complete helical revolution occurred every 60 ms (i.e. the shape is nearly identical at 0 and 60, 10 and 70, 20 and 80 ms), but the cell translated just 0.7 μm, or 29% of a wavelength, per revolution. Thus, there was substantial circumferential slip, as expected for propulsion in a dilute aqueous medium. For comparison, *Escherichia coli* swims at 30 μm s^{-1} in aqueous solutions (Purcell, 1977).

Discussion

The ultrastructure of *T. primitia* was examined here using electron cryotomography, and the results are summarized in Fig. 11A. Unique surface bowls dotted the outer membrane exterior. Novel hook-shaped appendages were aligned in parallel, face-to-face rows, generating macromolecular arcades striping the length of the cell's outer membrane sometimes, but not always, directly above the two juxtaposed PF. Fibrils extended from the cell tips. Periplasmic cones were found at the cell poles between the two membranes, and the flagella lay between two distinct periplasmic layers. The cytoplasm was clearly partitioned into distinct regions by membrane invaginations, storage granules and ribosome-excluding nucleoids.

In other organisms, familiar surface structures, like S-layers, fimbriae and fibrils, serve as protective coats, as platforms for adhesion and interaction with neighbours and hosts, and in motility (Fernandez and Berenguer, 2000; Moissl *et al*., 2005). While the incomplete coverage of the surface bowls and arcades argue against a protective role, the positioning of some hook arcades over the flagella suggests that they might be involved in motility. The surface bowls may be related to the taller and skinnier 'goblet' structures that cover the outer membrane of *Flexibacter polymorphus* (Ridgway *et al*., 1975; Ridgway, 1977). Symbiotic spirochetes are already known to attach to protozoa at their cell tips (Bloodgood and Fitzharris, 1976; Holt, 1978), so the tufts of fibrils seen here decorating the tips might be involved in some such interaction. Most fibrils are known to extend from the outer membrane, but some originate from the inner membrane (White, 2007). Here some fibrils were seen to extend into and perhaps all the way through the periplasmic cones, which may serve to anchor features for cell attachment, stabilize the poles during motility or determine shape.

Normally, Gram-negative bacteria have only one peptidoglycan layer linked to proteins from both the outer and inner membrane. The unique motility strategy of spirochetes, however, presents a structural challenge because the rotating PF must somehow be contained. The discovery of two periplasmic layers in *T. primitia* offers an elegant solution: the flagella rotate within an apparently structurally reinforced space. The inner periplasmic layer probably consists of peptidoglycan, as MotB of the flagellar stators (which is present in *Treponema*) is known to bind to peptidoglycan for stability (Berg, 2003). The composition of the outer periplasmic layer is unknown, but the presence of such a layer may help explain the formation of patterns seen previously in the outer membranes of the related species *S. aurantia*, *Spirochaeta litoralis* and *Treponema microdentium* (Holt, 1978).

While in all spirochetes, motility seems to be driven by rotation of the PF, the existing models for how this happens can be distinguished by whether or not flagellar rotation causes changes in the overall shape of the cell. In spirochetes that swim by changing their shape, the flagella are presumably stiffer than the rest of the cell, so that as the flagella rotate, they force the cell to change shape. This model applies to *L. interrogans* and *B. burgdorferi*, for instance, which gyrate and bend as spiral and planar waves, respectively, propagate down their lengths (Berg *et al*., 1978; Goldstein and Charon, 1988; Goldstein *et al*., 1994; 1996). In spirochetes that do not change shape, such as *C. balbianii* and *S. aurantia*, the flagella

must be less stiff than the rest of the cell, as the flagella must continually flex and bend to rotate within their fixed but curved tunnel-like compartments (Berg, 1976; Berg and Turner, 1979). As *T. primitia* appears to maintain a constant helical shape as it swims, it must also fall into this second class.

How then do the PF generate thrust? One possibility (Berg, 1976) can be explained with the following analogies (see also the animation in Movie S6). Starting with a simple cylinder, suppose that a smaller 'roller' is positioned parallel to and alongside the cylinder, and is attached to it near its ends so that the roller can spin independently of the cylinder, much like a paint roller spins independently of its handle. Now if the cylinder and roller were encased within a tube, and there were friction between the outside of the roller and the inner surface of the tube, then as the roller spun, the cylinder and tube would begin to counter-rotate. If the tube were then immobilized by its environment, all the rotation of the roller would be transmitted to the inner cylinder, which would then 'roll' around within the fixed tube, just like a unicyclist attempting to ride up the walls of a tunnel. Now finally imagine that instead of being a simple cylinder, the inner 'core' was actually a rigid helix; then like a corkscrew penetrating a cork, its rotation would cause it to bore forward into the cork.

In the context of a bacterial cell, the core is called the PC and comprises everything at smaller radius than the roller, which is of course the PF, and the tube is called the OS, which comprises everything at higher radius. More specifically in the case of *T. primitia*, the PC would include the inner periplasmic layer, the inner membrane and everything they enclose. The OS would include the outer periplasmic layer, the outer membrane and all the surface features reported here. The flagellar motors at opposite ends of the cell are opposed, so when the PF rotate in opposite directions (one clockwise and the other counterclockwise, when viewed from outside the cell), they work together to rotate the PC within the OS (as can be seen in transverse section, i.e. Fig. 11A). As the PF are tethered to the PC by their motors at their ends and remain next to each other along their lengths in the middle of the cell, then like the roller and cylinder system described above, when the PF rotate, they cannot 'roll' across the surface of the PC, but rather spin in place, like a car tire slipping on ice. In contrast, the PF might grip the OS, causing it to roll around the PC, or reciprocally, if movement of the OS is hindered by the environment, rotation of the PF might cause the PC to roll within the OS (brown and blue arrows in Fig. 11B). If the cell were in a gel-like medium, e.g. 1% methylcellulose or dilute agar, because the PC has a rigid helical shape, it will 'drill' forward when surrounded by environmental fibres like a corkscrew through a cork (red and green arrows in Fig. 11C) (Berg and Turner, 1979). If, however, the cell were in a dilute aqueous medium (more like the situation in Fig. 10), thrust would be generated by the slantwise slip of segments of the helical body relative to the external medium, just as thrust is generated by slantwise slip of segments of flagellar filaments for ordinary, flagellated bacteria (Berg, 1993), but progress would be slower. If both flagellar motors changed their directions of rotation, the cell would back up. If only one motor changed its direction of rotation, the cell would likely stop.

Our structural and swimming observations support this model of motility for *T. primitia*. In addition to protecting the membranes from rotation of the PF, the two periplasmic layers might facilitate counter-rotation of the PC and OS. The OS did not appear to be wrapped

tightly around the PC, consistent with the idea that these might counter-rotate. Forward thrust would be enhanced by friction between the environment and the OS, but the OS must also be able to slip forward through the medium with the PC. The hook arcades and surface bowls might serve this purpose, resisting rotation within the environment, but not forward movement because of their left-handed helical arrangements, which mimic the shape of the cell itself like long rudders below a ship.

One potential problem with the model is that counter-rotation of the two membranes would presumably prevent efflux channels from forming. Efflux channels are either transitory or longer-lived alignments of inner and outer membrane channels and periplasmic adapters that create 'stovepipes' to expel cytoplasmic contents (Piddock, 2006). Sequence similarities suggest that some efflux channels like NorM, AcrB, AcrA and TolC are present in *Leptospira*, *Borrelia* and *Treponema* species (data not shown). If the OS and PC counter-rotate, such channels would break. Also, if the fibrils connect to the periplasmic cone and inner membrane, then counter-rotation would strain this connection. The cone might stabilize the periplasm at the ends of the cell, so that fibrils and efflux channels could assemble and function there. The cone would then not connect rigidly to the outer periplasmic layer, but rather 'cap' it at the poles. The presumably fluid outer membrane would rotate with the outer periplasmic layer at the midcell, but move less at the cell poles above the cones, shearing as necessary in between to maintain its integrity.

These hypotheses suggest specific experiments. The sequence of the *T. primitia* genome is nearing completion. The fibrils, surface bowls and hook arcades should be identifiable as major components of purified OSs. Once methods to introduce genetic alterations are established, deletion mutants may elucidate the functions of these structures. Fluorescent tags on some external structure and an inner membrane protein or the flagellum might reveal whether the OS does in fact rotate with respect to the PC. Fluorescent tags on efflux channels should reveal whether or not they are in fact confined to the poles, and overexpression of such channels might cause them to mislocalize to the midcell, linking the OS and PC there and disrupting motility. It is already clear, however, that the ultrastructure and motility of *T. primitia* are richly complex.

Experimental procedures

Cell growth and grid preparation

Treponema primitia is an anaerobic organism that can survive for only a short time in the atmosphere. Cultures of *T. primitia* strain ZAS-2 were grown at 23°C in sealed culture tubes containing 4YACo medium under an atmosphere of 80% H_2 and 20% CO_2 as described previously (Leadbetter *et al*., 1999), and harvested during log-growth at an OD of ~0.6. To prevent aggregation in high-salt solutions, 10 nm colloidal gold was pre-treated with 5% BSA for 30 min. It was then concentrated fivefold and 5 μl was applied to glow-discharged, carbon-coated R 2/2 quantifoil grids and dried. ZAS-2 is an obligate anaerobe, but can tolerate atmospheric conditions for about 20 min, so grids were frozen in small batches. A small volume of cell solution was removed from a culture tube with a syringe. And 5 μl of the solution was applied to a grid. The grids were manually blotted on the reverse side of the applied liquid and frozen using a gravity plunger. Centrifugation even at low speed (4000 *g*)

lysed or disrupted the outer membranes, thus centrifugation was avoided. Automated blotting using a Vitrobot (FEI Company) was avoided because blotting on both sides of the grid caused catastrophic rupture of the outer membrane, so grids were manually blotted to minimize trauma.

Electron tomography data collection and 3-D reconstruction

The data collection and reconstruction process was described previously (Murphy *et al*., 2006). Single-axis tilt series were collected using a 300 keV FEI Polara FEG TEM automated by UCSF Tomo (Zheng *et al*., 2004). Typically, tilts were incremented 1° from −63° to 63°. The magnification was 22 500 (0.98 nm pixel^{-1}) and the total dose was ~110 e^{-}/Å^2, distributed according to the 1/cos scheme. Tomograms were reconstructed using IMOD (Kremer *et al*., 1996) and binned twofold (1.96 nm pixel^{-1}). Reconstruction handedness was confirmed through analyses of 3-D test samples with known front–back, left–right and up–down relationships.

Image processing

Reconstructions were segmented manually using Amira (Mercury Computing Systems). To display the fibrils, the region of the fibrils was segmented to create a mask, which was then applied to the volume file. The fibrils were displayed as an isosurface. Surface bowls and hooks were averaged by computationally extracting individual particles, aligning, and averaging them using the Bsoft image-processing package (Heymann, 2001). One hundred-fold symmetry was imposed on the surface bowls to smooth the reconstructions. The true symmetry of the surface bowls, if any, is unknown. Amira was used to estimate all measurements. To measure periplasmic density, the volume of one cell interior to the outer membrane was segmented. A surface map was generated and then smoothed. Density normal to this one surface was measured at each vertex of the surface triangles using a customized Amira module. The density was averaged to display density versus periplasmic depth. Measurements were taken over more than 25 000 pixels, corresponding to about 1% of the total surface area of a cell.

Light microscopy

Phase-contrast images of swimming cells were captured at 100 Hz using a high-speed AxioCamHS digital camera mounted on an AxioPlan 2 microscope (Carl Zeiss).

Supplementary Material

Refer to Web version on PubMed Central for supplementary material.

Acknowledgements

We thank H. Jane Ding for creating an Amira module for analysis, Dylan Morris for Fig. 11C and Everett Kane for creating the animation. This work was supported in part by NIH Grants P01 G66521 and R01 AI067548 to G.J.J., DOE Grant DE-FG02-04ER63785 to G.J.J., a Searle Scholar Award to G.J.J., NSF Grants DEB-0321753 and EF-0523267 to J.R.L., NIH Grant AI016478 to H.C.B., NIH Graduate Fellowship F31 EB 004179 to G.E.M., and gifts to Caltech from the Ralph M. Parsons Foundation, the Agouron Institute, and the Gordon and Betty Moore Foundation.

References

Berg HC. How spirochetes may swim. J Theor Biol. 1976; 56:269–273. [PubMed: 1271822]

Berg, HC. Random Walks in Biology. Princeton, NJ: Princeton University Press; 1993.

Berg HC. The rotary motor of bacterial flagella. Annu Rev Biochem. 2003; 72:19–54. [PubMed: 12500982]

Berg HC, Turner L. Movement of microorganisms in viscous environments. Nature. 1979; 278:349–351. [PubMed: 370610]

Berg HC, Bromley DB, Charon NW. Leptospiral motility. Symp Soc Gen Microbiol. 1978; 28:285–294.

Bloodgood RA, Fitzharris TP. Specific associations of prokaryotes with symbiotic flagellate protozoa from the hindgut of the termite *Reticulitermes* and the wood-eating roach *Cryptocercus*. Cytobios. 1976; 17:103–122. [PubMed: 1036325]

Breznak JA, Switzer JM. Acetate synthesis from H(2) plus CO(2) by termite gut microbes. Appl Environ Microbiol. 1986; 52:623–630. [PubMed: 16347157]

Cleveland LR, Grimstone AV. The fine structure of the flagellate *Mixotricha paradoxa* and its associated micro-organisms. Proc R Soc Lond. 1964; B159:668–686.

Fernandez LA, Berenguer J. Secretion and assembly of regular surface structures in Gram-negative bacteria. FEMS Microbiol Rev. 2000; 24:21–44. [PubMed: 10640597]

Goldstein SF, Charon NW. Motility of the spirochete Leptospira. Cell Motil Cytoskeleton. 1988; 9:101–110. [PubMed: 3282685]

Goldstein SF, Charon NW. Multiple-exposure photographic analysis of a motile spirochete. Proc Natl Acad Sci USA. 1990; 87:4895–4899. [PubMed: 2367518]

Goldstein SF, Charon NW, Kreiling JA. *Borrelia burgdorferi* swims with a planar waveform similar to that of eukaryotic flagella. Proc Natl Acad Sci USA. 1994; 91:3433–3437. [PubMed: 8159765]

Goldstein SF, Buttle KF, Charon NW. Structural analysis of the *Leptospiraceae* and *Borrelia burgdorferi* by high-voltage electron microscopy. J Bacteriol. 1996; 178:6539–6545. [PubMed: 8932310]

Graber JR, Leadbetter JR, Breznak JA. Description of *Treponema azotonutricium sp. nov.* and *Treponema primitia sp. nov.*, the first spirochetes isolated from termite guts. Appl Environ Microbiol. 2004; 70:1315–1320. [PubMed: 15006748]

Heymann JB. Bsoft: image and molecular processing in electron microscopy. J Struct Biol. 2001; 133:156–169. [PubMed: 11472087]

Holt SC. Anatomy and chemistry of spirochetes. Microbiol Rev. 1978; 42:114–160. [PubMed: 379570]

Izard J, McEwen BF, Barnard RM, Portuese T, Samsonoff WA, Limberger RJ. Tomographic reconstruction of treponemal cytoplasmic filaments reveals novel bridging and anchoring components. Mol Microbiol. 2004; 51:609–618. [PubMed: 14731266]

Jensen GJ, Briegel A. How electron cryotomography is opening a new window into prokaryotic ultrastructure. Curr Opin Cell Biol. 2007; 17:260–267.

Kremer JR, Mastronarde DN, McIntosh JR. Computer visualization of three-dimensional image data using IMOD. J Struct Biol. 1996; 116:71–76. [PubMed: 8742726]

Leadbetter JR, Schmidt TM, Graber JR, Breznak JA. Acetogenesis from H2 plus CO2 by spirochetes from termite guts. Science. 1999; 283:686–689. [PubMed: 9924028]

Lefman J, Zhang P, Hirai T, Weis RM, Juliani J, Bliss D, et al. Three-dimensional electron microscopic imaging of membrane invaginations in *Escherichia coli* overproducing the chemotaxis receptor Tsr. J Bacteriol. 2004; 186:5052–5061. [PubMed: 15262942]

Li, C.; Motaleb, MA.; Sal, M.; Goldstein, SF.; Charon, NW. Gyrations, rotations, periplasmic flagella: the biology of spirochete motility. In: Saier, MH., Jr; Garcia-Lara, J., editors. The Spirochetes Molecular and Cellular Biology. Norfolk: Horizon Press; 2001. p. 11-22.

Lucic V, Forster F, Baumeister W. Structural studies by electron tomography: from cells to molecules. Annu Rev Biochem. 2005; 74:833–865. [PubMed: 15952904]

Moissl C, Rachel R, Briegel A, Engelhardt H, Huber R. The unique structure of archaeal 'hami', highly complex cell appendages with nano-grappling hooks. Mol Microbiol. 2005; 56:361–370. [PubMed: 15813730]

Murphy GE, Leadbetter JR, Jensen GJ. *In situ* structure of the complete *Treponema primitia* flagellar motor. Nature. 2006; 442:1062–1064. [PubMed: 16885937]

Nakamura S, Adachi Y, Goto T, Magariyama Y. Improvement in motion efficiency of the spirochete *Brachyspira pilosicoli* in viscous environments. Biophys J. 2006; 90:3019–3026. [PubMed: 16415052]

Piddock LJ. Multidrug-resistance efflux pumps – not just for resistance. Nat Rev Microbiol. 2006; 4:629–636. [PubMed: 16845433]

Purcell EM. Life at low Reynolds number. Am J Phys. 1977; 45:3–11.

Ridgway HF. Ultrastructural characterization of goblet-shaped particles from the cell wall of *Flexibacter polymorphus*. Can J Microbiol. 1977; 23:1201–1213. [PubMed: 907917]

Ridgway HF, Wagner RM, Dawsey WT, Lewin RA. Fine structure of the cell envelope layers of *Flexibacter polymorphus*. Can J Microbiol. 1975; 21:1733–1750. [PubMed: 1201515]

Warnecke F, Luginbuhl P, Ivanova N, Ghassemian M, Richardson TH, Stege JT, et al. Metagenomic and functional analysis of hindgut microbiota of a wood-feeding higher termite. Nature. 2007; 450:560–565. [PubMed: 18033299]

White, D. The Physiology and Biochemistry of Prokaryotes. New York: Oxford University Press; 2007.

Zhang P, Bos E, Heymann J, Gnaegi H, Kessel M, Peters PJ, Subramaniam S. Direct visualization of receptor arrays in frozen-hydrated sections and plunge-frozen specimens of *E. coli* engineered to overproduce the chemotaxis receptor Tsr. J Microsc. 2004; 216:76–83. [PubMed: 15369487]

Zheng QS, Braunfeld MB, Sedat JW, Agard DA. An improved strategy for automated electron microscopic tomography. J Struct Biol. 2004; 147:91–101. [PubMed: 15193638]

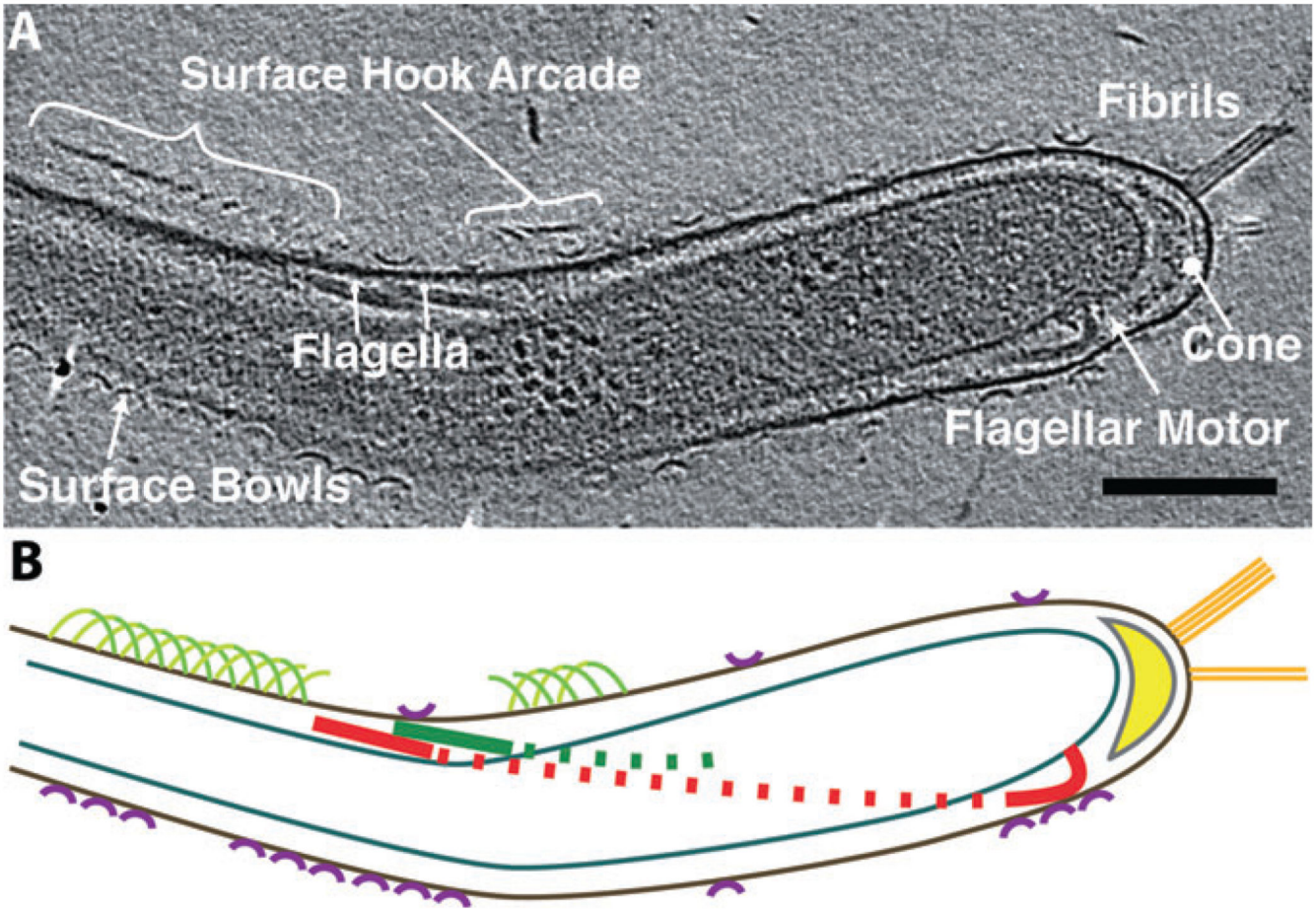

Fig. 1. Electron cryotomographic reconstruction of *T. primitia*

A. 10 nm section through the reconstruction of a frozen-hydrated *T. primitia* cell (cell #1). Surface bowls (magenta) dot the outer membrane surface. The surface hook arcades (chartreuse) wind atop the cell. Fibrils (orange) extend from the cell tip above a periplasmic cone (yellow). PF (red and green) wrap around the cell. Scale bar 200 nm.

B. Cartoon rendering of A. The same colours are used for all the figures and movies.

Fig. 2. Surface views of cell #1

A–D. Four side views of cell #1, incrementally rotated by 90°.

E. View of the cell tip showing the periplasmic cone underlying the fibrils.

F. View from the midcell region.

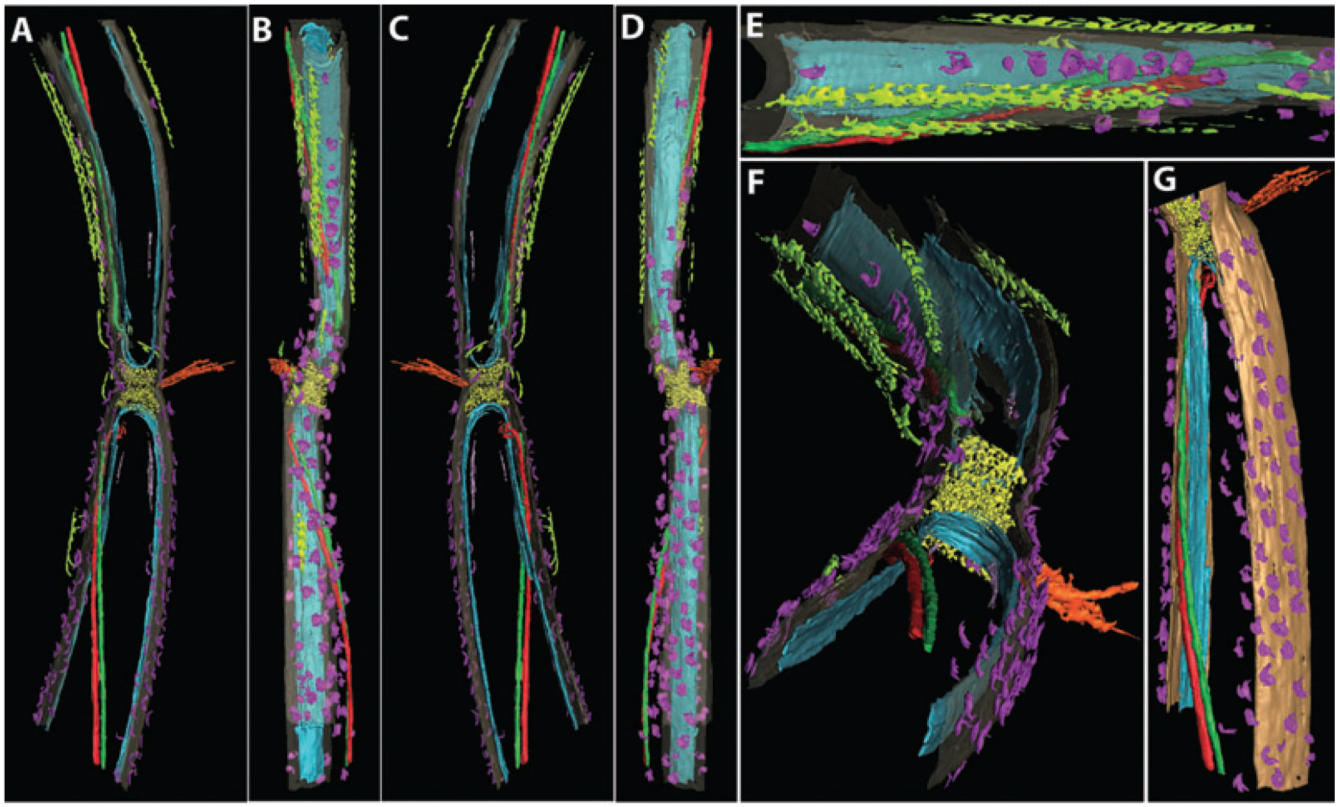

Fig. 3. Surface views of a connected cell

A–D. Four side views of a connected cell (cell #2), incrementally rotated by 90°.

E. A magnified view of the top cell showing the nearly matched winding of the hook arcades over the flagella.

F. Oblique view similar to A showing multiple arcades around the cell, including one pair over the flagella and two others not above flagella.

G. Oblique view similar to D, showing the only instance in segmented cells where the surface bowls appeared in helical rows around the cell.

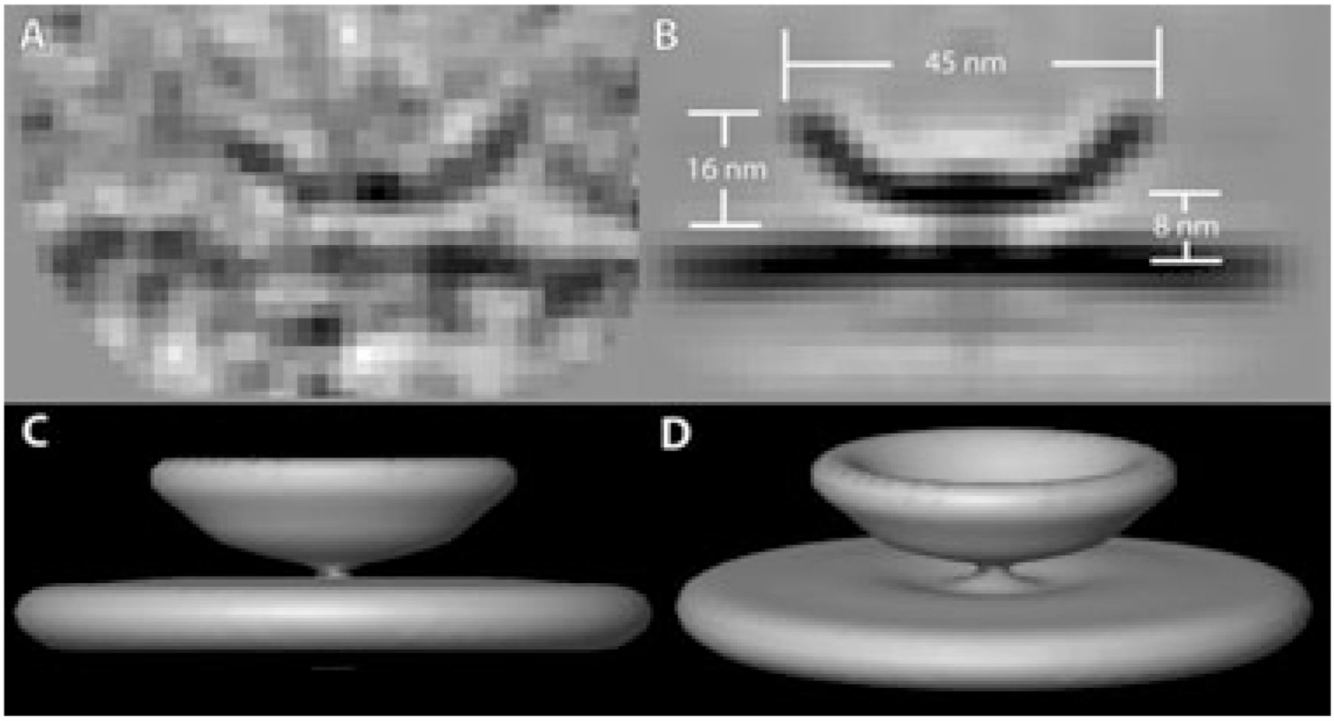

Fig. 4. Surface bowls

A. Axial section through the 3-D reconstruction of a single surface bowl.

B. Axial slice through the symmetrized average of many bowls.

C. Side view of the symmetrized average.

D. Inclined view.

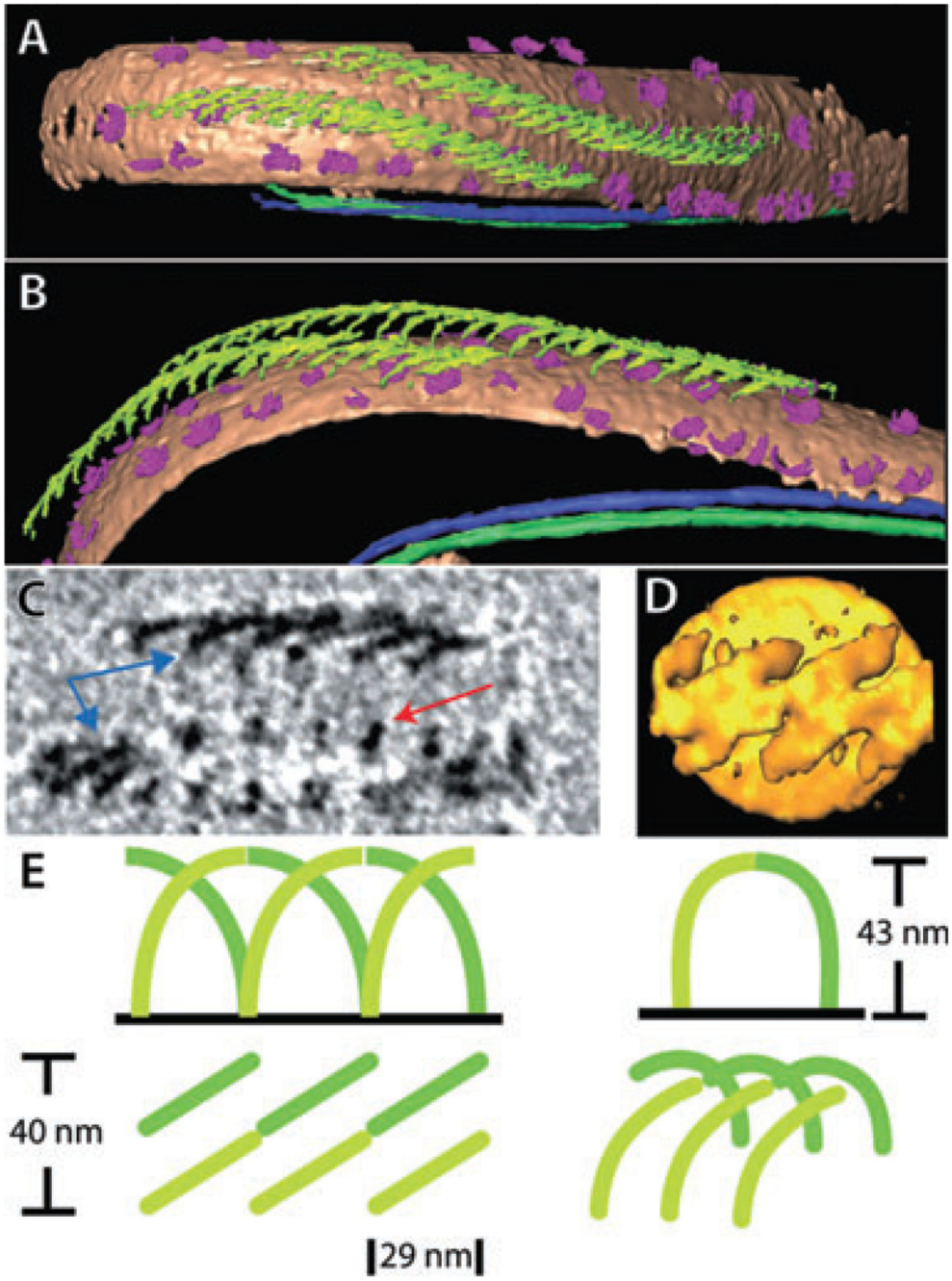

Fig. 5. The hook arcade

A. Top view of cell #3, whose outer membrane had ruptured and separated somewhat from the PC, yielding the clearest reconstruction of a pair of hook arcades.

B. Oblique view of the same hook arcades.

C. 4 nm section through the 3-D reconstruction, showing individual hook pillars (red arrow) and elsewhere the top of the arcade (blue arrows).

D. A top view of the average of several hook arcade sections.

E. Cartoon drawing of the individual hooks that constitute an arcade. A hook arches over and abuts an opposite hook two pillars down.

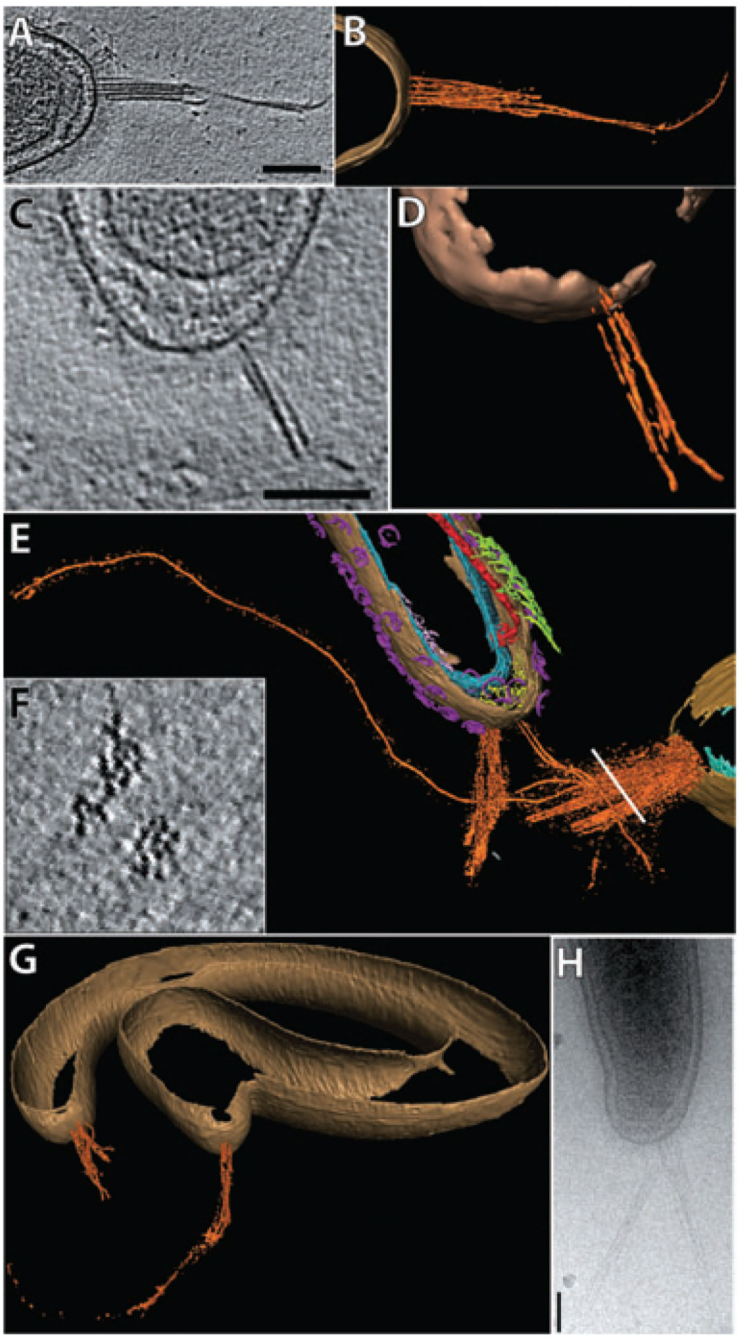

Fig. 6. Polar fibrils

A. 2 nm section through the tip of cell #4, showing several fibrils extending from the tip.

B. 3-D view of cell #4, showing an isosurface of the fibrils and a manual segmentation of the outer membrane.

C. 2 nm section through the tip of cell #3, showing what appears to be continuous density from the fibrils through the periplasmic cone to the inner membrane.

D. 3-D view of cell #3 as in B.

E. Isosurface of the fibrils extending from cell #1 (top) and from an additional cell (#1a, lower left) present in the same reconstruction. The fibrils in cell #1a are much more numerous, touch each other, and one fibril is ~1.6 μm long.

F. Cross section through the bundle of fibrils from cell #1a taken at the white line in E. The individual fibrils are ~6 nm thick.

G. 3-D view of cell #5, showing fibrils extending from both tips.

H. Projection image of the tip of cell #6, showing forked fibrils. (all scale bars are 100 nm)

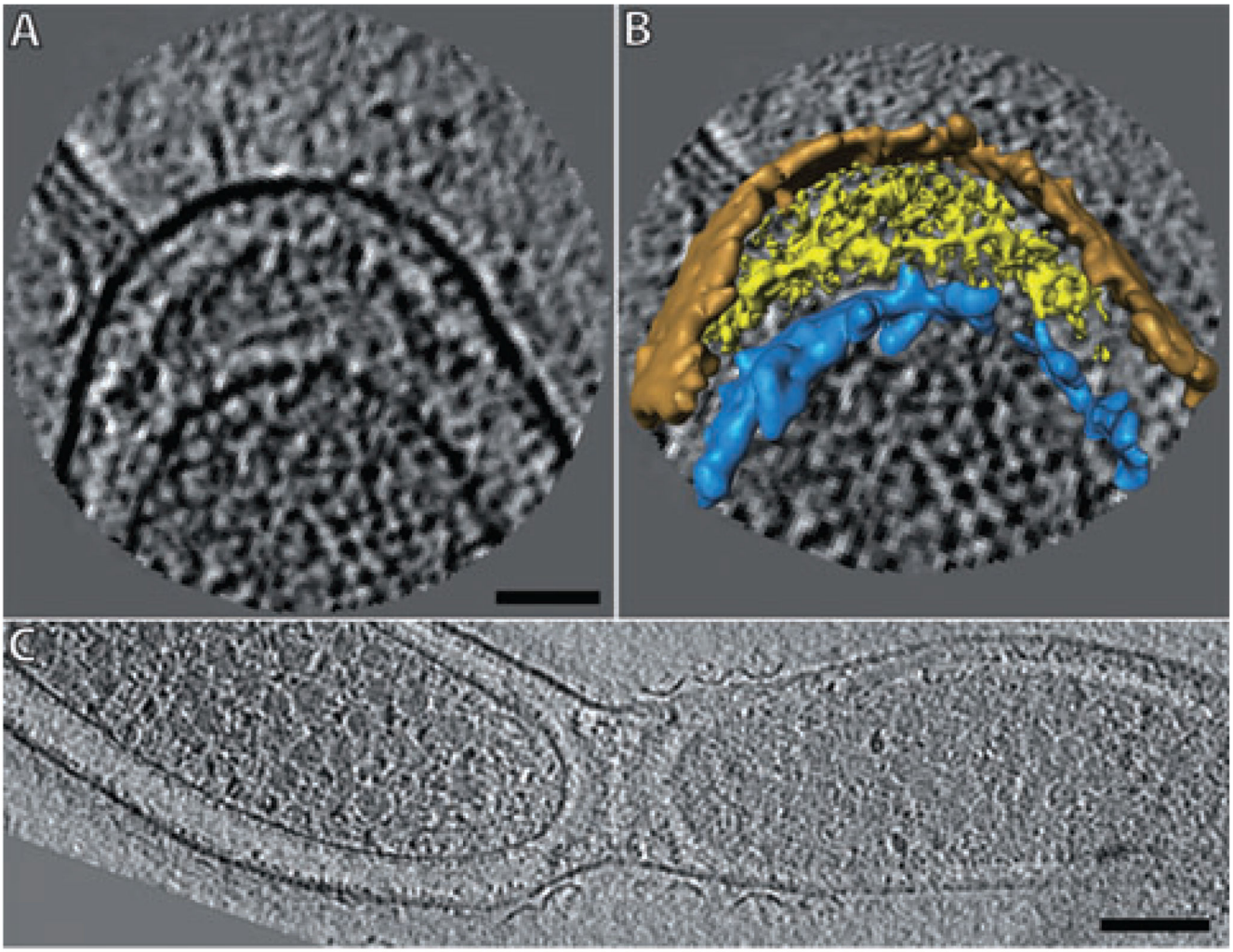

Fig. 7. Periplasmic cone

A. 2 nm section through the periplasmic cone of cell #1 (scale bar is 40 nm).

B. 3-D view of cell #1, showing an isosurface of the periplasmic cone and manual segmentations of the outer and inner membranes.

C. 6 nm section through two connected cells (#7 left and #7a right). The two periplasmic cones abut each other in the shape of an hourglass. Cell #7 was also noteworthy, because its cytoplasm was packed with ~30-nm-wide, spherical bodies (scale bar is 100 nm).

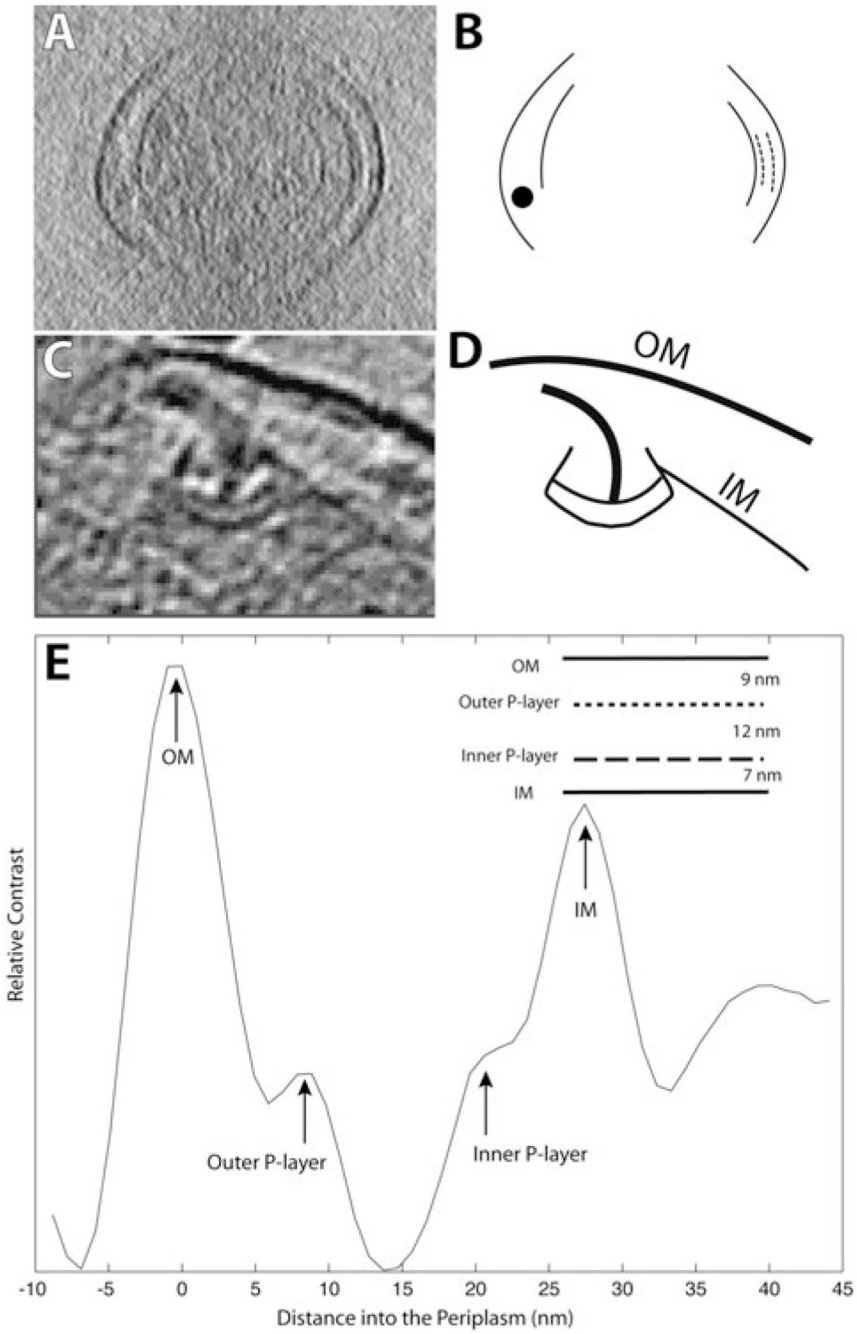

Fig. 8. Inner and outer periplasmic layers

A. 10 nm section through cell #8, showing two distinct periplasmic layers on the right side. The flagellum is at the bottom left. See Movie S4.

B. Cartoon guide to A.

C. 10 nm section through a region around the flagellar motor, showing the bulge of the periplasm near the motor.

D. Cartoon guide to C.

E. Average density of the periplasm as a function of distance into the cell from the outer membrane. The outer and inner periplasmic layers (‘P-layers’) are manifest by the smaller peaks between the two membranes.

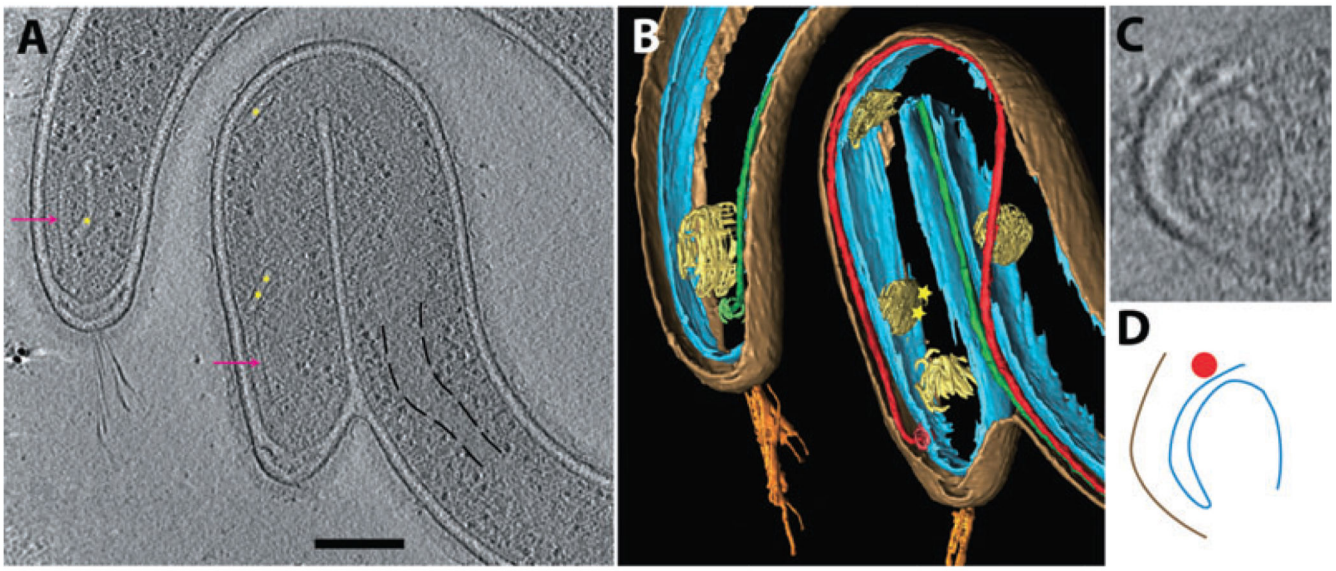

Fig. 9. Cytoplasmic structures

A. 6 nm section through cell #5 showing internal membranes (gold stars), probable chemotaxis receptor arrays (pink arrows) and ribosome-excluding regions (one example region delineated by black dashed lines). Scale bar is 200 nm.

B. Manual segmentation of cell #5. The membranes in the cytoplasm are flattened sacs near the inner membrane.

C. Inclined, interpolated 6 nm section through the membrane sac marked with double gold stars in A and B that appears to be an invagination of the inner membrane.

D. Cartoon tracing of the membranes in C.

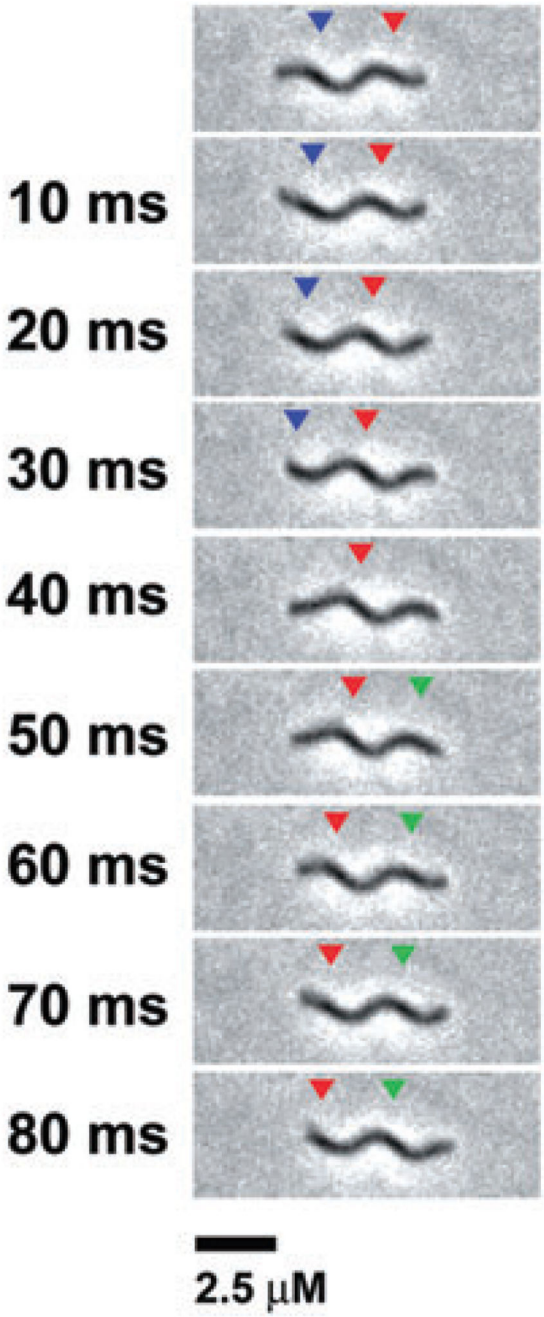

Fig. 10. A swimming *T. primitia* cell

Swimming cells were observed in a light microscope. Sequential frames of a single cell are pictured, showing that the cell maintains a constant helical shape as it swims. Arrows point to cell segments located in the focal plane. The cells swim at 12 μm s^{-1} in this buffer. See also Movie S5 for the complete movie.

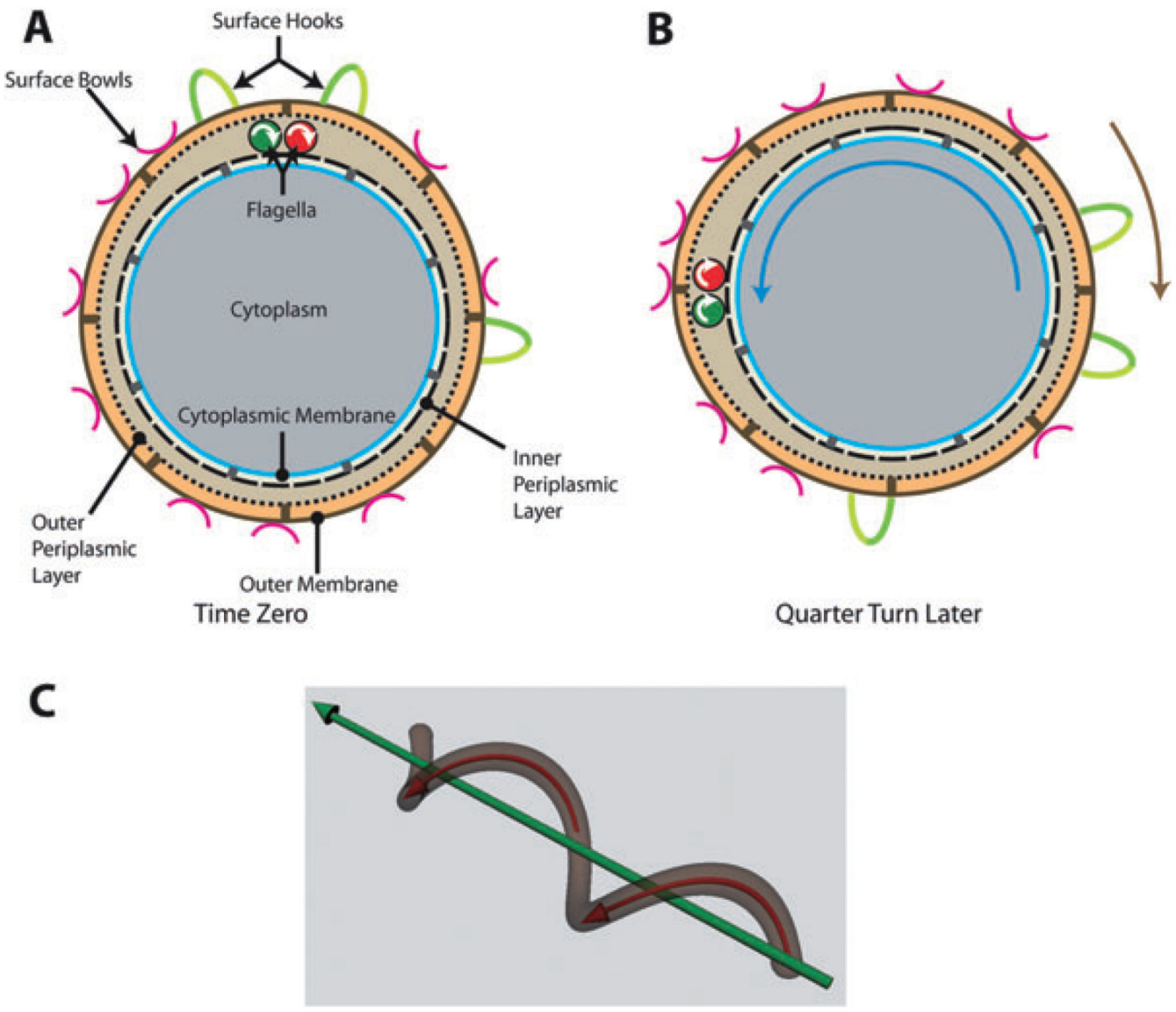

Fig. 11. Model of *T. primitia* ultrastructure and motility

A. Schematic cross section with labelled components at an imagined point (time ‘zero’) when the flagella are rotating clockwise (white arrows). The relative sizes of the cell thickness and the surface structures are to scale.

B. Same cross section a quarter turn later.

C. Oblique view of whole cell. Friction between the flagella and the OS (outer periplasmic layer and outer membrane) may cause the OS to rotate clockwise (brown arrow). In contrast, the PC (the inner periplasmic layer and inner membrane) must remain approximately fixed with respect to the flagella, because they are attached at the position of the motor. Friction of the OS against the environment may then cause the entire cell to roll counterclockwise (blue arrow). The helical cell would then drill itself forward like a corkscrew (red and green arrows).